
Beyond 1-WL with Local Ego-Network Encodings

Anonymous Author(s)

Anonymous Affiliation

Anonymous Email

Abstract

Identifying similar network structures is key to capture graph isomorphisms and learn representations that exploit structural information encoded in graph data. This work shows that ego-networks can produce a structural encoding scheme for arbitrary graphs with greater expressivity than the Weisfeiler-Lehman (1-WL) test. We introduce IGEL, a preprocessing step to produce features that augment node representations by encoding ego-networks into sparse vectors that enrich Message Passing (MP) Graph Neural Networks (GNNs) beyond 1-WL expressivity. We describe formally the relation between IGEL and 1-WL, and characterize its expressive power and limitations. Experiments show that IGEL matches the empirical expressivity of state-of-the-art methods on isomorphism detection while improving performance on seven GNN architectures.

1 Introduction

Novel approaches for representation learning on graph structured data have appeared in recent years [1]. Graph neural networks can efficiently learn representations that depend both on the graph structure and node and edge features from large-scale graph datasets. The most popular choice of architecture is the Message Passing Graph Neural Network (MP-GNN). In MP-GNNs, a node is represented by iteratively aggregating local feature ‘messages’ from its neighbors.

Despite being successfully applied in a wide variety of domains [2–6], there is a limit on the representational power of MP-GNNs provided by the computationally efficient Weisfeiler-Lehman (1-WL) test for checking graph isomorphism [7, 8]. Establishing this connection has led to a better theoretical understanding of the performance of MP-GNNs and many possible generalizations [9–13].

To improve the expressivity of MP-GNNs, recent methods have extended the vanilla message-passing mechanism in various ways. For example, using higher order k -vertex tuples [8] leading to k -WL generalizations, introducing relative positioning information for network vertices [14], propagating messages beyond direct neighborhoods [15], using concepts from algebraic topology [16], or combining sub-graph information in different ways [17–25]. All aforementioned approaches (which we review in more detail in Appendix A) improve expressivity by extending MP-GNNs architectures, often evaluating on standardized benchmarks [26–29]. However, identifying the optimal approach on novel domains remains unclear and requires costly architecture search.

In this work, we show that incorporating simple ego-network encodings already boosts the expressive power of MP-GNNs beyond the 1-WL test, while keeping the benefits of efficiency and simplicity. We present **IGEL**, an **I**nductive **G**raph **E**ncoding of **L**ocal information, which in its basic form extends node attributes with histograms of node degrees at different distances. The **IGEL** encodings can be computed as a pre-processing step irrespective of model architecture.

Theoretically, we formally prove that the **IGEL** encoding is no less expressive than the 1-WL test, and provide examples that show that it is more expressive than 1-WL. We also identify expressivity upper-bounds for graphs that are indistinguishable using state of the art methods. Experimentally, we assess the performance of seven model architectures enriched with **IGEL** encodings on five tasks and ten graph data sets, and find that it consistently improves downstream model performance.

2 IGEL: Ego-Networks As Sparse Inductive Representations

Given a graph $G = (V, E)$, we define $n = |V|$ and $m = |E|$, $d_G(v)$ is the degree of a node v in G and d_{\max} is the maximum degree. For $u, v \in V$, $l_G(u, v)$ is their shortest distance, and $\text{diam}(G) = \max(l_G(u, v) \mid u, v \in V)$ is the diameter of G . Double brackets $\{\{\cdot\}\}$ denote a lexicographically-ordered multi-set, $\mathcal{E}_v^\alpha \subseteq G$ is the α -depth ego-network centered on v , and $\mathcal{N}_G^\alpha(v)$ is the set of neighbors of v in G up to distance α , i.e., $\mathcal{N}_G^\alpha(v) = \{u \mid u \in V \wedge l_G(u, v) \leq \alpha\}$.

Algorithm 1 shows the 1-WL test, where hash maps a multi-set to an equivalence class shared by all nodes with matching multi-set encodings after a 1-WL iteration. The output of 1-WL is \mathbb{N}^n —mapping each node to a color, bounded by n distinct colors if each node is uniquely colored. k -higher order variants of the WL test (denoted k -WL) operate on k -tuples of vertices, such that colors are assigned to k -vertex tuples. If two graphs G_1, G_2 are not distinguishable by the k -WL test (that is, their coloring histograms match), they are k -WL equivalent—denoted $G_1 \equiv_{k\text{-WL}} G_2$. Due to the hashing step, 1-WL does not preserve distance information in the encoding, and minor changes in the structure of the network (removing one edge) may dramatically change node-level representations. IGEL addresses both limitations, improving expressivity in the process.

2.1 The IGEL Algorithm

Intuitively, IGEL encodes a vertex v with the multi-set of ordered degree sequences at each distance within \mathcal{E}_v^α . As such, IGEL is a variant of the 1-WL algorithm shown in Algorithm 1, executed for α steps with two modifications. First, the hashing step is removed and replaced by computing the union of multi-sets across steps (\cup); second, the iteration number is explicitly introduced in the representation—with the output multi-set e_v^α shown in Algorithm 2.

To be used as vertex features, the multi-set can be represented as a sparse vector $\text{IGEL}_{\text{vec}}^\alpha(v)$, where the frequency of a pair of distance λ and degree δ is contained on index $i = \lambda \cdot (d_{\max} + 1) + \delta$. Degrees greater than d_{\max} are capped to d_{\max} , with the resulting vector shown in Figure 1:

$$\text{IGEL}_{\text{vec}}^\alpha(v)_i = \left| \left\{ \{(\lambda, \delta) \in e_v^\alpha\} \right\} \right|$$

$$\text{for } \lambda \cdot (d_{\max} + 1) + \delta = i.$$

$G_1 = (V_1, E_1)$ and $G_2 = (V_2, E_2)$ are IGEL-equivalent for α if the sorted multi-set containing node representations is the same for G_1 and G_2 :

$$G_1 \equiv_{\text{IGEL}}^\alpha G_2 \iff \left\{ \{e_{v_1}^\alpha : \forall v_1 \in V_1\} \right\} = \left\{ \{e_{v_2}^\alpha : \forall v_2 \in V_2\} \right\}.$$

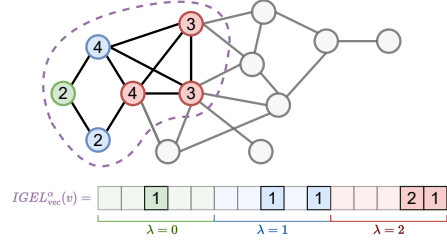


Figure 1: IGEL encoding of the green vertex. Dashed region denotes \mathcal{E}_v^α ($\alpha = 2$). The green vertex is at distance 0, blue vertices at 1 and red vertices at 2. Labels show degrees in \mathcal{E}_v^α . The frequency of (λ, δ) tuples forming $\text{IGEL}_{\text{vec}}^\alpha(v)$ is: $\{(0, 2) : 1, (1, 2) : 1, (1, 4) : 1, (2, 3) : 2, (2, 4) : 1\}$.

71

Algorithm 1 1-WL (Color refinement).

Input: $G = (V, E)$
 1: $c_v^0 := \text{hash}(\{\{d_G(v)\}\}) \forall v \in V$
 2: **do**
 3: $c_v^{i+1} := \text{hash}(\{\{c_u^i : \forall_{u \neq v} u \in \mathcal{N}_G^1(v)\}\})$
 4: **while** $c_v^i \neq c_v^{i-1}$
Output: $c_v^i : V \rightarrow \mathbb{N}$

Algorithm 2 IGEL Encoding.

Input: $G = (V, E), \alpha : \mathbb{N}$
 1: $e_v^0 := \{\{(0, d_G(v))\}\} \forall v \in V$
 2: **for** $i := 1; i += 1$ **until** $i = \alpha$ **do**
 3: $e_v^i := \cup(e_v^{i-1},$
 4: $\{\{(i, d_{\mathcal{E}_G^\alpha(v)}(u))$
 5: $\forall u \in \mathcal{N}_G^\alpha(v) \mid l_G(u, v) = i\})$
 6: **end for**
Output: $e_v^\alpha : V \rightarrow \{\{\mathbb{N}, \mathbb{N}\}\}$

Space complexity. IGEL's worst case space complexity is $\mathcal{O}(\alpha \cdot n \cdot d_{\max})$, conservatively assuming that every node will require d_{\max} parameters at every α depth from the center of the ego-network.

Time complexity. For IGEL, each vertex has d_{\max} neighbors where the α iterations imply traversing through geometrically larger ego-networks with $(d_{\max})^\alpha$ vertices, upper bounded by m . Thus IGEL's time complexity follows $\mathcal{O}(n \cdot \min(m, (d_{\max})^\alpha))$, with $\mathcal{O}(n \cdot m)$ when $\alpha \geq \text{diam}(G)$, when implemented as BFS, for which we provide further details in Appendix F.

78 3 Theoretical and Experimental Findings

79 First, we analyze IGEL’s expressive power with respect to 1-WL and recent improvements. Second,
80 we measure the impact of IGEL as an additional input to enrich existing MP-GNN architectures.

81 3.1 Expressivity: Which Graphs are IGEL-Distinguishable?

82 In this section, we discuss the increased expressivity of IGEL with respect to 1-WL, and identify
83 expressivity upper-bounds for graphs that are indistinguishable under MATLANG and the 3-WL test.

84 — **Relationship to 1-WL.** IGEL is more powerful than 1-WL following Lemma 1 (as shown
85 in Appendix C) and Lemma 2 (as shown below):

87 **Lemma 1.** *IGEL is at least as expressive than 1-WL. That is, for any pair of graphs G_1, G_2 such
88 that $G_1 \not\equiv_{1-WL} G_2$ are distinguished by 1-WL in k iterations, $G_1 \not\equiv_{IGEL}^\alpha G_2$ for $\alpha = k + 1$.*

91 **Lemma 2.** *There exist graphs that IGEL can distinguish but that 1-WL cannot distinguish.*

93 *Proof.* For example, any two d -regular graphs with equal cardinality are indistinguishable by
94 1-WL (as shown in Appendix B), but IGEL can distinguish some of them. A graph is d -regular
95 if all nodes have degree d . Figure 2 shows two d -regular graphs where 1-WL (Algorithm 1)
96 assigns the same color for all nodes, stabilizing after one iteration. In contrast, IGEL ($\alpha = 1$)
97 counts different frequencies for four structures, hence distinguishing between both graphs.
98
99
100
101
102

103 — **Expressivity upper bounds.** We identify an expressivity upper bound for IGEL, which fails to
104 distinguish Strongly Regular Graphs with equal parameters (Theorem 1, see Appendix E for details):

106 **Definition 1.** *A n -vertex d -regular graph is strongly regular—denoted $SRG(n, d, \beta, \gamma)$ —if adjacent
107 vertices have β vertices in common, and non-adjacent vertices have γ vertices in common.*

108 **Theorem 1.** *IGEL cannot distinguish SRGs when $n, d,$ and β are the same, and between any value of
109 γ (same or otherwise). IGEL when $\alpha = 1$ can only distinguish SRGs with different values of $n, d,$
110 and β , while IGEL when $\alpha = 2$ can only distinguish SRGs with different values of n and d .*

111 Our findings show that IGEL is a powerful permutation-equivariant representation (see Lemma 3),
112 capable of distinguishing 1-WL equivalent graphs as shown in Figure 2—which as cospectral graphs,
113 are known to be distinguishable in strictly more powerful MATLANG sub-languages than 1-WL [12].
114 Additionally, the upper bound on SRGs is a hard ceiling on expressivity since SRGs are known to
115 be indistinguishable by 3-WL [31]. IGEL shares the experimental upper-bound of expressivity of
116 methods like GNNML3 [20]. Furthermore, IGEL can provably reach comparable expressivity on
117 SRGs with respect to sub-graph methods implemented within MP-GNN architectures (see Appendix E,
118 subsection E.1), such as Nested GNNs [19] and GNN-AK [23], which are known to be not less
119 powerful than 3-WL, and ESAN when using ego-networks with root-node flags as subgraph sampling
120 policy (EGO+) [24], which is as powerful as the 3-WL test on SRGs (see [24], Prop. 3).

121 3.2 Experimental Evaluation

122 We evaluate $IGEL_{vec}^\alpha(v)$ to produce architecture-agnostic vertex features on five tasks: graph classification,
123 isomorphism detection, graphlet counting, link prediction, and node classification.

124 **Experimental Setup.** We introduce IGEL on graph classification, isomorphism and graphlet counting,
125 comparing the performance of adding/removing IGEL on six GNN architectures following [20]. We
126 also evaluate IGEL on link prediction against transductive baselines, and on node classification as
127 additional feature in MLPs without message-passing. Appendix G describes experimentation details.

128 **Notation.** The following formatting denotes significant (as per paired t-tests) **positive**, *negative*, and
129 insignificant differences after introducing IGEL, with the best results per task / dataset underlined.

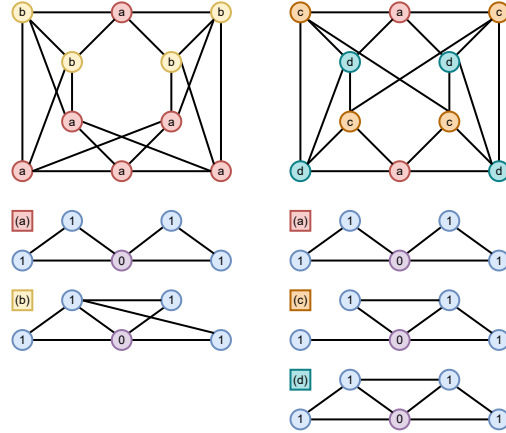


Figure 2: IGEL encodings for two Cospectral 4-regular graphs from [30]. IGEL distinguishes 4 kinds of structures within the graphs (associated with every node as a, b, c, and d). The two graphs can be distinguished since the encoded structures and their frequencies do not match.

Table 1: Per-model graph classification accuracy metrics on TU data sets. Each cell shows the average accuracy of the model and data set in that row and column, with IGEL (left) and without IGEL (right).

Model	Enzymes	Mutag	Proteins	PTC
MLP	41.10>26.18 [◇]	87.61>84.61 [◇]	75.43~75.01	64.59>62.79 [◇]
GCN	54.48>48.60 [◇]	89.61>85.42 [◇]	75.67>74.50 [*]	65.76~65.21
GAT	54.88~54.95	90.00>86.14 [◇]	73.44>70.51 [◇]	66.29~66.29
GIN	54.77>53.44 [*]	89.56~88.33	73.32>72.05 [◇]	61.44~60.21
Chebnet	61.88~62.23	91.44>88.33 [◇]	74.30>66.94 [◇]	64.79~63.87
GNNML3	61.42<62.79 [◇]	92.50>91.47 [*]	75.54>62.32 [◇]	64.26<66.10 [◇]

* $p < 0.01$, ◇ $p < 0.0001$

Table 2: Mean \pm stddev of best IGEL configuration and state-of-the-art results reported on [15, 18, 19, 21, 23, 24] with best performing baselines underlined.

Model	Mutag	Proteins	PTC
IGEL (ours)	92.5 \pm 1.2	75.7 \pm 0.3	66.3 \pm 1.3
<i>k</i> -hop [15] [†]	87.9 \pm 1.2 [◇]	75.3 \pm 0.4	—
GSN [18] [†]	92.2 \pm 7.5	76.6 \pm 5.0	68.2 \pm 7.2
NGNN [19] [†]	87.9 \pm 8.2	74.2 \pm 3.7	—
ID-GNN [21] [†]	93.0 \pm 5.6	77.9 \pm 2.4 [*]	62.5 \pm 5.3
GNN-AK [23] [†]	91.7 \pm 7.0	77.1 \pm 5.7	67.7 \pm 8.8
ESAN [24] [†]	91.1 \pm 7.0	76.7 \pm 4.1	69.2 \pm 6.5

†: Results as reported by [15, 18, 19, 21, 23, 24].

130 — **Graph Classification.** Table 1 shows graph classification results on the TU molecule data sets [27].
 131 We evaluate differences in mean accuracy between 10 runs with (left) / without (right) IGEL. We do
 132 not tune network hyper-parameters and establish statistical significance through paired t-tests, with
 133 $p < 0.01$ (*) and $p < 0.0001$ (◇). Our results show that IGEL in the Mutag and Proteins data sets
 134 improves the performance of all MP-GNN models, including GNNML3. On the Enzymes and PTC
 135 data sets, results are mixed: excluding GNNML3, IGEL either significantly improves accuracy (on
 136 MLPNet, GCN, and GIN on Enzymes), or does not have a negative impact on performance.

137 Table 2 compares IGEL results from Table 1 with reported results for state-of-the-art 1-WL expressive
 138 MP-GNNs. Results are comparable to IGEL except where highlighted in color. Overall, when
 139 comparing IGEL and best performing baselines, only differences with ID-GNN on Proteins are
 140 statistically significant (using p -value threshold $p < 0.01$, where ID-GNN shows $p = 0.009$).

141 — **Isomorphism Detection & Graphlet Counting.** Adding IGEL to the six models in Table 1 on the
 142 EXP [32] isomorphism detection yields significant improvements: all GNN models distinguish all
 143 non-isomorphic yet 1-WL equivalent EXP graph pairs with IGEL vs. 50% accuracy without IGEL (i.e.
 144 random guessing). Additionally, IGEL significantly improves GNN graphlet-counting performance
 145 on three graphlet types in the RandomGraph data set [33]. We provide further details in Appendix H.

146 — **Link Prediction & Node Classification.** We test IGEL on edge / node level tasks to assess its use
 147 as a baseline in non-GNN settings. On a transductive link prediction task, we train DeepWalk [34]
 148 style embeddings of IGEL encodings rather than node identities on the Facebook and CA-AstroPh
 149 graphs [35]. IGEL-derived embeddings outperform transductive baselines on link prediction as an
 150 edge-level binary classification task, measuring **0.976** vs. 0.968 (Facebook) and **0.984** vs. 0.937 (CA-
 151 AstroPh) AUC comparing IGEL vs. node2vec [36]. On multi-label node classification on PPI [37],
 152 we train an MLP (e.g. no message passing) with node features and IGEL encodings. Our MLP shows
 153 better micro-F1 (0.850) when $\alpha = 1$ than MP-GNN architectures such as GraphSAGE (0.768, as
 154 reported in [38]), but underperforms compared to a 3-layer GAT (**0.973** micro-F1 from [38]).

155 — **Experimental Summary.** Introducing IGEL yields comparable performance to state-of-the-art
 156 methods without architectural modifications—including when compared to strong baseline models
 157 focused on WL expressivity such as GNNML3, GSN, Nested GNNs, ID-GNN, GNN-AK or ESAN.
 158 Furthermore, IGEL achieves this at a lower computational cost, in comparison for instance with
 159 GNNML3, which requires a $\mathcal{O}(n^3)$ eigen-decomposition step to introduce spectral channels. Finally,
 160 IGEL can also be used in transductive settings (link prediction) as well as node-level tasks (node
 161 classification) and outperform strong transductive baselines or enhance models without message-
 162 passing, such as MLPs. As such, we believe IGEL is an attractive baseline with a clear relationship to
 163 the 1-WL test that improves MP-GNN expressivity without the need for costly architecture search.

164 4 Conclusions

165 We presented IGEL, a novel vertex representation algorithm on unattributed graphs allowing MP-
 166 GNN architectures to go beyond 1-WL expressivity. We showed that IGEL is related and more
 167 expressive than the 1-WL test, and formally proved an expressivity upper bound on certain families
 168 of Strongly Regular Graphs. Finally, our experimental results indicate that introducing IGEL in
 169 existing MP-GNN architectures yield comparable performance to state-of-the-art methods, without
 170 architectural modifications and at lower computational costs than other approaches.

References

- 171
- 172 [1] Michael M. Bronstein, Joan Bruna, Taco Cohen, and Petar Veličković. Geometric deep learning:
173 Grids, groups, graphs, geodesics, and gauges. *ArXiv*, abs/2104.13478, 2021. 1
- 174 [2] Rex Ying, Ruining He, Kaifeng Chen, Pong Eksombatchai, William L Hamilton, and Jure
175 Leskovec. Graph convolutional neural networks for web-scale recommender systems. In
176 *Proceedings of the 24th ACM International Conference on Knowledge Discovery & Data
177 Mining*, pages 974–983, 2018. 1
- 178 [3] David K Duvenaud, Dougal Maclaurin, Jorge Iparraguirre, Rafael Bombarell, Timothy Hirzel,
179 Alan Aspuru-Guzik, and Ryan P Adams. Convolutional networks on graphs for learning
180 molecular fingerprints. In *Advances in Neural Information Processing Systems*, 2015.
- 181 [4] Justin Gilmer, Samuel S. Schoenholz, Patrick F. Riley, Oriol Vinyals, and George E. Dahl.
182 Neural message passing for quantum chemistry. In *Proceedings of the 34th International
183 Conference on Machine Learning (ICML)*, volume 70, page 1263–1272, 2017.
- 184 [5] Bidisha Samanta, Abir De, Gourhari Jana, Vicenç Gómez, Pratim Chattaraj, Niloy Ganguly, and
185 Manuel Gomez-Rodriguez. NEVAE: A deep generative model for molecular graphs. *Journal of
186 Machine Learning Research*, 21(114):1–33, 2020.
- 187 [6] Peter Battaglia, Razvan Pascanu, Matthew Lai, Danilo Jimenez Rezende, and Koray
188 Kavukcuoglu. Interaction networks for learning about objects, relations and physics. In
189 *Advances in Neural Information Processing Systems*, 2016. 1
- 190 [7] Keyulu Xu, Weihua Hu, Jure Leskovec, and Stefanie Jegelka. How powerful are graph neural
191 networks? In *International Conference on Learning Representations*, 2019. 1
- 192 [8] Christopher Morris, Martin Ritzert, Matthias Fey, William L. Hamilton, Jan Eric Lenssen,
193 Gaurav Rattan, and Martin Grohe. Weisfeiler and Leman go neural: Higher-order graph neural
194 networks. *Thirty-Third AAAI Conference on Artificial Intelligence*, 33(01):4602–4609, 2019. 1
- 195 [9] Martin Grohe. *Descriptive Complexity, Canonisation, and Definable Graph Structure Theory*.
196 Lecture Notes in Logic. Cambridge University Press, 2017. 1
- 197 [10] Robert Brijder, Floris Geerts, Jan Van Den Bussche, and Timmy Weerwag. On the expressive
198 power of query languages for matrices. *ACM Trans. Database Syst.*, 44(4), 2019.
- 199 [11] Pablo Barceló, Egor V. Kostylev, Mikael Monet, Jorge Pérez, Juan Reutter, and Juan Pablo
200 Silva. The logical expressiveness of graph neural networks. In *International Conference on
201 Learning Representations*, 2020.
- 202 [12] Floris Geerts. On the expressive power of linear algebra on graphs. *Theory of Computing
203 Systems*, 65:1–61, 2021. 3
- 204 [13] Christopher Morris, Yaron Lipman, Haggai Maron, Bastian Rieck, Nils M Kriege, Martin Grohe,
205 Matthias Fey, and Karsten Borgwardt. Weisfeiler and Leman go machine learning: The story so
206 far. *arXiv preprint arXiv:2112.09992*, 2021. 1
- 207 [14] Jiaxuan You, Rex Ying, and Jure Leskovec. Position-aware graph neural networks. In *Proceed-
208 ings of the 36th International Conference on Machine Learning*, volume 97, pages 7134–7143.
209 PMLR, 2019. 1
- 210 [15] Giannis Nikolentzos, George Dasoulas, and Michalis Vazirgiannis. k-hop graph neural networks.
211 *Neural Networks*, 130:195–205, 2020. 1, 4, 7
- 212 [16] Cristian Bodnar, Fabrizio Frasca, Nina Otter, Yuguang Wang, Pietro Liò, Guido F Montufar,
213 and Michael Bronstein. Weisfeiler and Lehman go cellular: CW networks. In *Advances in
214 Neural Information Processing Systems*, 2021. 1
- 215 [17] Haggai Maron, Heli Ben-Hamu, Hadar Serviansky, and Yaron Lipman. Provably powerful
216 graph networks. In *Advances in Neural Information Processing Systems*, 2019. 1
- 217 [18] Giorgos Bouritsas, Fabrizio Frasca, Stefanos Zafeiriou, and Michael M. Bronstein. Improving
218 graph neural network expressivity via subgraph isomorphism counting, 2021. 4, 7
- 219 [19] Muhan Zhang and Pan Li. Nested graph neural networks. *Advances in Neural Information
220 Processing Systems*, 34, 2021. 3, 4, 7
- 221 [20] Muhammet Balcilar, Pierre Héroux, Benoit Gaüzère, Pascal Vasseur, Sébastien Adam, and Paul
222 Honeine. Breaking the limits of message passing graph neural networks. In *Proceedings of the
223 38th International Conference on Machine Learning (ICML)*, 2021. 3, 7, 11, 12, 13

- 224 [21] Jiaxuan You, Jonathan M Gomes-Selman, Rex Ying, and Jure Leskovec. Identity-aware graph
225 neural networks. In *Thirty-Fifth AAAI Conference on Artificial Intelligence*, volume 35, pages
226 10737–10745, 2021. 4, 7
- 227 [22] Dylan Sandfelder, Priyesh Vijayan, and William L Hamilton. Ego-gnns: Exploiting ego
228 structures in graph neural networks. In *IEEE International Conference on Acoustics, Speech
229 and Signal Processing (ICASSP)*, pages 8523–8527. IEEE, 2021. 7
- 230 [23] Lingxiao Zhao, Wei Jin, Leman Akoglu, and Neil Shah. From stars to subgraphs: Uplifting any
231 GNN with local structure awareness. In *International Conference on Learning Representations*,
232 2022. 3, 4, 7
- 233 [24] Beatrice Bevilacqua, Fabrizio Frasca, Derek Lim, Balasubramaniam Srinivasan, Chen Cai,
234 Gopinath Balamurugan, Michael M. Bronstein, and Haggai Maron. Equivariant subgraph
235 aggregation networks. In *International Conference on Learning Representations*, 2022. 3, 4, 7
- 236 [25] Pan Li, Yanbang Wang, Hongwei Wang, and Jure Leskovec. Distance encoding: Design
237 provably more powerful neural networks for graph representation learning. In *Advances in
238 Neural Information Processing Systems*, volume 33, pages 4465–4478, 2020. 1, 7
- 239 [26] Weihua Hu, Matthias Fey, Marinka Zitnik, Yuxiao Dong, Hongyu Ren, Bowen Liu, Michele
240 Catasta, and Jure Leskovec. Open graph benchmark: Datasets for machine learning on graphs.
241 *arXiv preprint arXiv:2005.00687*, 2020. 1
- 242 [27] Christopher Morris, Nils M. Kriege, Franka Bause, Kristian Kersting, Petra Mutzel, and Marion
243 Neumann. Tudataset: A collection of benchmark datasets for learning with graphs. In *ICML
244 2020 Workshop on Graph Representation Learning and Beyond (GRL+ 2020)*, 2020. 4
- 245 [28] Jiaxuan You, Zhitao Ying, and Jure Leskovec. Design space for graph neural networks. In
246 *Advances in Neural Information Processing Systems*, pages 17009–17021, 2020.
- 247 [29] Vijay Prakash Dwivedi, Chaitanya K Joshi, Thomas Laurent, Yoshua Bengio, and Xavier
248 Bresson. Benchmarking graph neural networks. *arXiv preprint arXiv:2003.00982*, 2020. 1
- 249 [30] Edwin R Van Dam and Willem H Haemers. Which graphs are determined by their spectrum?
250 *Linear Algebra and its Applications*, 373:241–272, 2003. 3
- 251 [31] Vikraman Arvind, Frank Fuhlbrück, Johannes Köbler, and Oleg Verbitsky. On Weisfeiler-Leman
252 invariance: Subgraph counts and related graph properties. *Journal of Computer and System
253 Sciences*, 113:42–59, 2020. 3
- 254 [32] Ralph Abboud, İsmail İlkan Ceylan, Martin Grohe, and Thomas Lukasiewicz. The surprising
255 power of graph neural networks with random node initialization. In *Proceedings of the Thirtieth
256 International Joint Conference on Artificial Intelligence*, pages 2112–2118, 2021. 4, 11
- 257 [33] Zhengdao Chen, Lei Chen, Soledad Villar, and Joan Bruna. Can graph neural networks count
258 substructures? In *Advances in Neural Information Processing Systems*, 2020. 4, 12, 13
- 259 [34] Bryan Perozzi, Rami Al-Rfou, and Steven Skiena. Deepwalk: Online learning of social repre-
260 sentations. In *Proceedings of the 20th ACM SIGKDD International Conference on Knowledge
261 Discovery and Data Mining*, pages 701–710, 2014. 4
- 262 [35] Jure Leskovec and Andrej Krevl. SNAP Datasets: Stanford large network dataset collection,
263 2014. URL <http://snap.stanford.edu/data>. 4
- 264 [36] Aditya Grover and Jure Leskovec. Node2vec: Scalable feature learning for networks. In
265 *Proceedings of the 22nd ACM SIGKDD International Conference on Knowledge Discovery and
266 Data Mining*, pages 855–864, 2016. 4
- 267 [37] Will Hamilton, Zhitao Ying, and Jure Leskovec. Inductive representation learning on large
268 graphs. In *Advances in Neural Information Processing Systems 30*, 2017. 4
- 269 [38] Petar Veličković, Guillem Cucurull, Arantxa Casanova, Adriana Romero, Pietro Liò, and Yoshua
270 Bengio. Graph attention networks. In *International Conference on Learning Representations*,
271 2018. 4
- 272 [39] Petar Veličković. Message passing all the way up. In *ICLR 2022 Workshop on Geometrical and
273 Topological Representation Learning*, 2022. 7
- 274 [40] Anonymous. Rethinking the expressive power of GNNs via graph biconnectivity. In *Submitted
275 to The Eleventh International Conference on Learning Representations*, 2023. under review. 7

A Relation with Previous Works

In the past few years, many different approaches have been developed for improving the expressivity of MP-GNNs. Here we review the works that are more related to IGEL. For a more detailed overview augmented message-passing methods for graph representation learning, see [39].

In *k*-hop MP-GNNs (*k*-hop) [15] the authors propose to propagate messages beyond immediate vertex neighbors, effectively using ego-network information in the vertex representation. Their proposed algorithm requires to extract neighborhood sub-graphs and to perform message-passing on each sub-graph, which has an exponential cost on the number of hops *k* both at pre-processing and at each iteration (epoch). In contrast, IGEL only requires a single pre-processing step that can be cached once computed.

Distance Encoding GNNs (DE-GNN) [25] also propose to improve MP-GNN by using extra node features by encoding distances to a subset of *p* nodes. The features obtained by DE-GNN are similar to IGEL when conditioning the subset to size $p = 1$ and using a distance encoding function with $k = \alpha$. However, these features are not strictly equivalent to the IGEL features, since within the ego-network the node degrees can be smaller than the actual degrees, and they are more expensive to compute. DE-GNN needs to compute power iterations of the entire adjacency matrix, which is more expensive and does not exploit network sparsity.

Graph Substructure Networks (GSNs) [18] incorporate hand-crafted topological features by counting local substructures (such as the presence of cliques or cycles). GSNs require expert knowledge on what features are relevant for a given task and depart from the original MP-GNN in their architecture. We show that IGEL reaches comparable performance using a general encoding for ego-networks and without altering the original message-passing mechanism.

GNNML3 [20] proposes a way to perform message passing in spectral-domain with a custom frequency profile. While this approach achieves good performance on graph classification, it requires an expensive preprocessing step for computing the eigendecomposition of the graph Laplacian and $\mathcal{O}(k)$ -order tensors to achieve *k*-WL expressiveness, which does not scale to large graphs.

More recently, a series of methods formulate the problem of representing vertices or graphs as aggregations over sub-graphs. The sub-graph information is pooled or introduced during message-passing at an additional cost that varies depending on each architecture. Consequently, they require generating the subgraphs (or effectively replicating the nodes of every subgraph of interest) and pay an additional overhead due to the aggregation. These approaches include Ego-GNNs [22], Nested GNNs (NGNNs) [19], GNN-as-Kernel (GNN-AK) [23], Identity-aware GNNs (ID-GNNs) [21].

Ego-GNNs perform message-passing over the ego-graphs of all the nodes in a graph, and subsequently perform aggregation. They provide empirical evidence of a superior expressive power than the classical 1-WL. ID-GNNs embed each node incorporating identity information in the GNN and apply rounds of heterogeneous message passing; NGNNs perform a two-level GNN using rooted sub-graphs and consider a graph as a bag of sub-graphs; GNN-AK uses a very similar idea, but as the authors describe, it sets the number of layers to the number of iterations of 1-WL; Compared to all these methods IGEL only relies on an initial pre-processing step based on distances and degrees without having to run additional message passing iterations. Despite its simplicity, IGEL performs competitively, as we show in Table 2.

Equivariant Subgraph Aggregation Networks (ESAN) [24] also propose to encode bags of subgraphs and show that such an encoding can lead to a better expressive power. In the case of the ego-networks policy (EGO), ESAN is strongly related with IGEL. Interestingly, as described in concurrent work [40], the implicit encoding of the pairwise distance between nodes, plus the degree information which can be extracted via aggregation are fundamental to provide a theoretical justification of ESAN. In this work, we directly consider distances and degrees in the ego-network, explicitly providing the structural information encoded by more expressive GNN architectures. These similarities may explain why the performance of both methods is comparable, as shown in Table 2.

B 1-WL Expressivity and Regular Graphs

Remark 1 shows that 1-WL, as defined in Algorithm 1, is unable of distinguishing *d*-regular graphs: **Remark 1.** Let G_1 and G_2 be two *d*-regular graphs such that $|V_1| = |V_2|$. Tracing Algorithm 1, all vertices in V_1, V_2 share the same initial color due to *d*-regularity: $\forall v \in V_1 \cup V_2; c_v^0 = \text{hash}(\{d\})$.

329 *After the first color refinement iteration, consider the colorings of G_1 and G_2 :*

330

$$331 \text{---} \forall v_1 \in V_1; c_{v_1}^1 := \mathit{hash}(\{\{c_{u_1}^0 : \forall_{u_1 \neq v_1} u_1 \in \mathcal{N}_{G_1}^1(v_1)\}\}),$$

$$332 \text{---} \forall v_2 \in V_2; c_{v_2}^1 := \mathit{hash}(\{\{c_{u_2}^0 : \forall_{u_2 \neq v_2} u_2 \in \mathcal{N}_{G_2}^1(v_2)\}\}).$$

333

334 *Since $\forall v_1 \in V_1, v_2 \in V_2; d = |\mathcal{N}_{G_1}^1(v_1)| = |\mathcal{N}_{G_2}^1(v_2)|$, substituting $c_{v_1}^1, c_{v_2}^1$ in the next iteration*
 335 *step yields $\{\{\mathit{hash}(c_{v_1}^1) : \forall v_1 \in V_1\}\} = \{\{\mathit{hash}(c_{v_2}^1) : \forall v_2 \in V_2\}\}$. Thus, on any pair of d -regular*
 336 *graphs with equal cardinality, 1-WL stabilizes after one iteration produces equal colorings for all*
 337 *nodes on both graphs—regardless of whether G_1 and G_2 are isomorphic, as Figure 2 shows.*

338 C IGEL is At Least As Powerful as 1-WL

339 In this section we formally prove Lemma 1, i.e. that IGEL is at least as expressive as 1-WL. For this,
 340 we consider a variant of 1-WL which removes the hashing step. This modification can only increase
 341 the expressive power of 1-WL but makes it possible to directly compare with the encodings generated
 342 by IGEL. Intuitively, after k color refinement iterations, 1-WL considers nodes at k hops from each
 343 node, which is equivalent to running IGEL with $\alpha = k + 1$, so that the ego-networks include the
 344 information of all nodes that 1-WL would visit.

345 **Lemma 1.** *IGEL is at least as expressive than 1-WL. That is, for any pair of graphs G_1, G_2 such*
 346 *that $G_1 \not\equiv_{1-WL} G_2$ are distinguished by 1-WL in k iterations, $G_1 \not\equiv_{IGEL}^\alpha G_2$ for $\alpha = k + 1$.*

347 *Proof.* For convenience, let $c_v^{i+1} = \{\{c_v^i; c_v^i \forall_{u \neq v} u \in \mathcal{N}_G^1(v)\}\}$ be a recursive definition of Algorithm 1

348 where hashing is removed and $c_v^0 = \{\{d_G(v)\}\}$. Since the hash is no longer computed, the nested
 349 multi-sets contain strictly the same or more information as in the traditional 1-WL algorithm.

350 Consider two graphs $G_1 = (V_1, E_1)$ and $G_2 = (V_2, E_2)$. Let k be the minimum number of color
 351 refinement iterations such that $\exists v_1 \in V_1$ s.t. $\forall v_2 \in V_2, c_{v_1}^k \neq c_{v_2}^k$. For IGEL to be less expressive
 352 as 1-WL, it must hold that $G_1 \not\equiv_{1-WL} G_2 \Leftrightarrow G_1 \equiv_{IGEL}^\alpha G_2$. Thus, for any colors distinguished
 353 between the two graphs $c_{v_1}^k \neq c_{v_2}^k, \forall \alpha$ such that $e_{v_1}^\alpha = e_{v_2}^\alpha$. By construction of the 1-WL test,
 354 $c_{v_1}^k = \{\{\{\dots\{d_G(v_1)\}\}, \{d_G(u) \forall u \in \mathcal{N}_{G_1}^1(v_1)\}\dots\}$. For convenience, the multi-set of nested
 355 degree multi-sets can be rewritten as the union of degree multi-sets by introducing an indicator
 356 variable for the iteration number where a given degree is found:

$$\begin{aligned} c_{v_1}^k = & \left\{ \left\{ (d_G(v_1), 0) \right\} \right\} \cup \\ & \left\{ \left\{ (d_G(v_1), 1); (d_G(u), 1) \forall u \in \mathcal{N}_{G_1}^1(v) \right\} \right\} \cup \\ & \left\{ \left\{ (d_G(v_1), 2); (d_G(u), 2) \forall u \in \mathcal{N}_{G_1}^1(v); (d_G(w), 2) \forall w \in \mathcal{N}_{G_1}^2(u) \right\} \right\} \cup \dots \end{aligned}$$

357 At each step i , we introduce information about nodes up to distance i of v_1 . Furthermore, by
 358 construction, nodes will be visited on every subsequent iteration—i.e. for $c_{v_1}^2$, we will observe
 359 $(d_G(v_1), 2)$ exactly $d_G(v_1) + 1$ times, as its $d_G(v_1)$ neighbors $u \in \mathcal{N}_{G_1}^1(v)$ its degree in c_u^1 . This
 360 notation is equivalent or more expressive than 1-WL, as it keeps track of the refinement iteration at
 361 which a given degree is found.

362 Now consider the case in which $c_{v_1}^k \neq c_{v_2}^k$, and let $\alpha = k + 1$ so that IGEL considers degrees counting
 363 edges at k to $k + 1$ hops of v_1 and v_2 . We know that the color refinement algorithm has introduced
 364 information about nodes at a maximum distance k of v_1 and v_2 . Assume that $G_1 \equiv_{IGEL}^\alpha G_2$. By
 365 construction, this means that $\{\{e_{v_1}^\alpha : \forall v_1 \in V_1\}\} = \{\{e_{v_2}^\alpha : \forall v_2 \in V_2\}\}$. This presents a contradiction,
 366 as by construction all degrees and iteration counts (as per the distance) match, so $c_{v_1}^k = c_{v_2}^k$, and thus
 367 $G_1 \equiv_{1-WL} G_2$. Thus, $G_1 \not\equiv_{1-WL} G_2 \Leftrightarrow G_1 \not\equiv_{IGEL}^\alpha G_2$ for $\alpha = k + 1$. \square

D IGEL is Permutation Equivariant

Lemma 3. Given any $v \in V$ for $G = (V, E)$ and given a permuted graph $G' = (V', E')$ of G produced by a permutation of node labels $\pi : V \rightarrow V'$ such that $\forall v \in V \Leftrightarrow \pi(v) \in V'$, $\forall (u, v) \in E \Leftrightarrow (\pi(u), \pi(v)) \in E'$.

The IGEL representation is permutation equivariant at the graph level

$$\pi(\{e_{v_1}^\alpha, \dots, e_{v_n}^\alpha\}) = \{e_{\pi(v_1)}^\alpha, \dots, e_{\pi(v_n)}^\alpha\}.$$

The IGEL representation is permutation invariant at the node level

$$e_v^\alpha = e_{\pi(v)}^\alpha, \forall v \in G.$$

Proof. Note that e_v^α in Algorithm 2 can be expressed recursively as:

$$e_v^\alpha = \left\{ \left(l_{\mathcal{E}_v^\alpha}(u, v), d_{\mathcal{E}_v^\alpha}(u) \right) \mid \forall u \in \mathcal{N}_G^\alpha(v) \right\}.$$

Since IGEL only relies on node distances $l_G(\cdot, \cdot)$ and degree nodes $d_G(\cdot)$, and both $l_G(\cdot, \cdot)$ and $d_G(\cdot)$ are permutation invariant (and the node level) and equivariant (at the graph level) functions, the IGEL representation is permutation equivariant at the graph level, and permutation invariant at the node level. \square

E Proof of Theorem 1

In this appendix, we provide proof for Theorem 1, showing that IGEL cannot distinguish certain pairs of SRGs with equal parameters of n (cardinality), d (degree), β (shared edges between adjacent nodes), and γ (shared edges between non-adjacent nodes). Let $\{\cdot\}^d$ denote a repeated multi-set with d -times the cardinality of the items in the multi-set, and let $e_G^\alpha = \{e_v^\alpha : \forall v \in V\}$ be short-hand notation for the IGEL encoding of G , defined as the sorted multi-set containing IGEL encodings of all nodes in G .

Lemma 4. For any $G = \text{SRG}(n, d, \beta, \gamma)$, $\text{diam}(G) \leq 2$.

Note that by definition of SRGs, n affects cardinality while d and β control adjacent vertex connectivity at 1-hop. For γ , we have to consider two cases: when $\gamma \geq 1$ and when $\gamma = 0$:

— Let $\gamma \geq 1$: by definition, $\forall u, v \in V$ s.t. $(u, v) \notin E, \exists w \in V$ s.t. $(u, w) \in E \wedge (v, w) \in E$. Thus, $\forall (u, v) \in E, l_G(u, v) = 1$ and $\forall (u, v) \notin E, l_G(u, v) = 2$.

— Let $\gamma = 0$: $\forall u, v \in V$, if $(u, v) \notin E$ then $\nexists w \in V$ s.t. $(u, w) \in E \wedge (v, w) \in E$ as w is in common between u and v . Then, $\forall u, v, w \in V$ s.t. $(u, v) \in E, (u, w) \in E \Leftrightarrow (v, w) \in E$ —hence, only nodes and their neighbors can be in common. Thus: $\forall u, v \in V$ s.t. $u \neq v, l_G(u, v) = 1$.

Given both scenarios, we can conclude that for any $\gamma \in \mathbb{N}$, $\forall u, v \in V, l_G(u, v) \leq 2$ and thus $\text{diam}(G) \leq 2$. \square

Lemma 5. For any finite graph G , there is a finite range of $\alpha \in \mathbb{N}$ where IGEL encodings distinguish between different values of α . For values of α larger than the diameter of the graph (that is, $\alpha \geq \text{diam}(G)$), it holds that $e_v^\alpha = e_v^{\alpha+1}$ as $\mathcal{E}_v^\alpha = \mathcal{E}_v^{\alpha+1} = G$. \square

Proof. Per Lemma 4 and Lemma 5, SRGs have a maximum diameter of two, and IGEL encodings are equal for all $\alpha \geq \text{diam}(G)$. Thus, given $G = \text{SRG}(n, d, \beta, \gamma)$, only $\alpha \in \{1, 2\}$ produce different encodings of G . It can be shown that e_v^α can only distinguish different values of n, d and β , and $\text{IGEL}_{\text{enc}}^2$ can only distinguish values of n and d :

— Let $\alpha = 1$: $\forall v \in V, \mathcal{E}_v^1 = (V', E')$ s.t. $V' = \mathcal{N}_G^1(v)$. Since G is d -regular, v is the center of \mathcal{E}_v^1 , and has d -neighbors. By SRG's definition, the d neighbors of v have β shared neighbors with v each, plus an edge with v . Thus, for any SRGs G_1, G_2 where $n_1 = n_2, d_1 = d_2$, and $\beta_1 = \beta_2$, $e_{G_1}^1 = e_{G_2}^1$ produce equal encodings by expanding e_v^1 in Algorithm 2:

$$e_v^1 = \left\{ (0, d) \right\} \cup \left\{ (1, \beta + 1) \right\}^d$$

406 — Let $\alpha = 2$: $\forall v \in V, \mathcal{E}_v^2 = G$ as $\forall u \in V, u \in \mathcal{N}_G^2(v)$ when $\text{diam}(G) \leq 2$. G is d -regular, so
 407 $\forall v \in V, d = d_{\mathcal{E}_v^2}(v) = d_G(v)$. Thus, for any SRGs G_1, G_2 s.t. $n_1 = n_2$ and $d_1 = d_2$, $e_{G_1}^2 = e_{G_2}^2$,
 408 containing n equal e_v^2 encodings by expanding [Algorithm 2](#):

$$e_v^2 = \left\{ \{ (0, d) \} \cup \left\{ \{ (1, d) \} \right\}^d \cup \left\{ \{ (2, d) \} \right\}^{n-d-1} \right\}$$

409 Thus, IGEL cannot distinguish pairs of SRGs when n, d , and β are the same, and between any value
 410 of γ (equal or different between the pair). IGEL when $\alpha = 1$ can only distinguish SRGs with different
 411 values of n, d , and β , while IGEL when $\alpha = 2$ can only distinguish SRGs with different values of n
 412 and d . \square

413 We note that it is straightforward to extend IGEL so that different values of γ can be distinguished.
 414 We explore one possible extension in [subsection E.1](#).

415 E.1 Improving Expressivity on the γ Parameter

416 IGEL as presented is unable to distinguish between any values of γ in SRGs. However, IGEL can be
 417 trivially extended to distinguish between pairs of SRGs, bringing parity with methods such as the
 418 EGO+ policy in ESAN, NGNNs and GNN-AK.

419 Intuitively, IGEL is unable to distinguish γ because its (λ, δ) tuples are unable to represent relation-
 420 ships between vertices at different distances (i.e. the γ parameter). The structural feature definition
 421 may be extended to compute the degree between ‘distance layers’ in the sub-graphs, addressing this
 422 pitfall. This means modifying e_v^i in [Algorithm 2](#):

$$e_v^i = e_v^{i-1} \cup \left\{ \left\{ \rho(u, v) : \forall u \in \mathcal{N}_G^\alpha(v) \mid l_G(u, v) \in \{i, i+1\} \right\} \right\}$$

423 where:

$$\rho(u, v) = \left(l_{\mathcal{E}_v^\alpha}(u, v), d_{\mathcal{E}_v^\alpha}^0(u, v), d_{\mathcal{E}_v^\alpha}^1(u, v) \right)$$

424 and $d_G^p(u, v)$ generalizes $d_G(u)$ to count edges of u at a relative distance p of v in $G = (V, E)$:

$$d_G^p(u, v) = \left| \{ (u, w) \in E \mid w \in V \text{ s.t. } l_G(u, w) = l_G(u, v) + p \} \right|.$$

425 It can be shown that this definition of e_v^i is strictly more powerful distinguishing at SRGs following an
 426 expansion of [Algorithm 2](#) with $\alpha = 2$:

$$e_v^2 = \left\{ \{ (0, 0, d) \} \cup \left\{ \{ (1, \beta, \gamma) \} \right\}^d \cup \left\{ \{ (2, d - \gamma, 0) \} \right\}^{n-d-1} \right\}$$

427 *Proof.* For any $G = \text{SRG}(n, d, \beta, \gamma)$, $\forall v \in V, l_{\mathcal{E}_v^2}(v, v) = 0$ and there are d edges towards its
 428 neighbors—thus the root is encoded as $(0, 0, d)$. Each neighbor is at $l_{\mathcal{E}_v^2}(u, v) = 1$, with β edges
 429 among each other, and γ with vertices not adjacent to v —thus $(1, \beta, \gamma)$, where $d = 1 + \beta + \gamma$.
 430 By definition, every vertex $w \in V \text{ s.t. } (u, w) \notin E$ has γ neighbors shared with v , and d neighbors
 431 overall. Per [Lemma 4](#), the maximum diameter of G is two, hence $l_{\mathcal{E}_v^2}(v, w) = 2$ and for any w , the
 432 representation is $(2, d - \gamma, 0)$. \square

433 F Implementing IGEL through Breadth-First Search

434 The idea behind the IGEL encoding is to represent each vertex v by compactly encoding its cor-
 435 responding ego-network \mathcal{E}_v^α at depth α . The choice of encoding consists of a histogram of vertex
 436 degrees at distance $d \leq \alpha$, for each vertex in \mathcal{E}_v^α . Essentially, IGEL runs a Breadth-First Traversal up
 437 to depth α , counting the number of times the same degree appears at distance $d \leq \alpha$.

438 The algorithm shown in [Algorithm 2](#) showcases IGEL and its relationship to the 1-WL test. However,
 439 in a practical setting, it might be preferable to implement IGEL through Breadth-First Search (BFS).
 440 In [Algorithm 3](#), we show one such implementation that fits the time and space complexity described
 441 in [section 2](#):

Algorithm 3 IGEL Encoding (BFS).

```

Input:  $v \in V, \alpha \in \mathbb{N}$ 
1: toVisit := [] ▷ Queue of nodes to visit.
2: degrees := {} ▷ Mapping of nodes to their degrees.
3: distances := { $v : 0$ } ▷ Mapping of nodes to their distance to  $v$ 
4: while toVisit  $\neq \emptyset$  do
5:    $u := \text{toVisit.dequeue}()$ 
6:   currentDistance := distances[ $u$ ]
7:   currentDegree := 0
8:   for  $w \in u.\text{neighbors}()$  do
9:     if  $w \notin \text{distances}$  then
10:      distances[ $w$ ] := currentDistance + 1 ▷  $w$  is a new node 1-hop further from  $v$ .
11:    end if
12:    if distances[ $w$ ]  $\leq \alpha$  then
13:      currentDegree := currentDegree + 1 ▷ Count edges only within  $\alpha$ -hops.
14:      if  $w \notin \text{degrees}$  then ▷ Enqueue if  $w$  has not been visited.
15:        toVisit.append( $w$ )
16:      end if
17:    end if
18:  end for
19:  degrees[ $u$ ] := currentDegree ▷  $u$  is now visited: we know its degree and distance to  $v$ .
20: end while
21:  $e_v^\alpha = \{( \text{distances}[u], \text{degrees}[u] ) \mid \forall u \in \text{degrees.keys}()\}$ 
▷ Produce the multi-set of (distance, degree) pairs for all visited nodes.

```

Output: $e_v^\alpha : (\mathbb{N}, \mathbb{N}) \rightarrow \mathbb{N}$

442 Due to how we structure BFS to count degrees and distances in a single pass, each edge is processed
 443 twice—once for each node at end of the edge. It must be noted that when processing every $v \in V$, the
 444 time complexity is $\mathcal{O}(n \cdot \min(m, (d_{\max})^\alpha))$. However, the BFS implementation is also embarrassingly
 445 parallel, which means that it can be distributed over p processors with $\mathcal{O}(n \cdot \min(m, (d_{\max})^\alpha)/p)$
 446 time complexity.

447 G Experimental Settings And Procedures

448 In this section, we provide additional details of our experimental setting. We summarize our datasets
 449 and tasks in Table 6.

450 On graph-level tasks, we introduce IGEL encodings concatenated to existing vertex features into the
 451 best performing model configurations found by [20] without any hyper-parameter tuning (e.g. number
 452 of layers, hidden units, choice pooling and activation functions). We evaluate performance differences
 453 with and without IGEL on each task, data set and model on 10 independent runs, measuring statistical
 454 significance of the differences through paired t-tests.

455 On vertex and edge-level tasks, we report best performing configurations after hyper-parameter
 456 search. Each configuration is evaluated on 5 independent runs. We provide a breakdown of the best
 457 performing hyper-parameters in the section below.

458 G.1 Hyper-parameters and Experiment Details

459 Graph Level Experiments

460 We reproduce the benchmark of [20] without modifying model hyper-parameters for the tasks of
 461 Graph Classification, Graph Isomorphism Detection, and Graphlet Counting. For classification tasks,
 462 the 6 models in Table 2 are trained on binary / categorical cross-entropy objectives depending on the
 463 task. For Graph Isomorphism Detection, we train GNNs as binary classification models on the binary
 464 classification task on EXP [32], and identify isomorphisms by counting the number of graph pairs

Table 3: Values of α used when introducing IGEL in the best reported configuration for graphlet counting and graph classification tasks. The table is broken down by graphlet types (upper section) and graph classification tasks on the TU Datasets (bottom section).

	Chebnet	GAT	GCN	GIN	GNNML3	Linear	MLP
Star	2	1	2	1	1	2	1
Tailed Triangle	1	1	1	1	2	1	1
Triangle	1	1	1	1	1	1	1
4-Cycle	2	1	1	1	1	1	1
Custom Graphlet	2	1	1	1	2	2	2
Enzymes	1	2	2	1	2	2	2
Mutag	1	1	1	1	1	1	2
Proteins	2	2	2	1	2	1	1
PTC	1	1	2	1	1	2	2

465 for which randomly initialized MP-GNN models produce equivalent outputs on Graph8c¹². For the
 466 graphlet counting regression task on the RandomGraph data set [33], we train models to minimize
 467 Mean Squared Error (MSE) on the normalized graphlet counts³ for five types of graphlets.

468 On all tasks, we experiment with $\alpha \in \{1, 2\}$ and optionally introduce a preliminary linear transfor-
 469 mation layer to reduce the dimensionality of IGEL encodings. For every setup, we execute the same
 470 configuration 10 times with different seeds and compare runs introducing IGEL or not by measuring
 471 whether differences on the target metric (e.g. accuracy or MSE) are statistically significant as shown
 472 in Table 1 and Table 2. In Table 3, we provide the value of α that was used in our experimental
 473 results. Our results show that the choice of α depends on both the task and model type. We believe
 474 these results may be applicable to subgraph-based MP-GNNs, and will explore how different settings,
 475 graph sizes, and downstream models interact with α in future work.

476 *Reproducibility*– We will provide an additional repository with our changes to the original benchmark,
 477 including our modelling scripts, metadata, and experimental results.

478 Vertex and Edge-level Experiments

479 In this section we break down the best performing hyper-parameters on the Edge (link prediction)
 480 and Vertex-level (node classification) experiments.

481 *Link Prediction*– The best performing hyperparameter configuration on the Facebook graph including
 482 $\alpha = 2$, learning $t = 256$ component vectors with $e = 10$ walks per node, each of length $s = 150$ and
 483 $p = 8$ negative samples per positive for the self-supervised negative sampling. Respectively on the
 484 arXiv citation graph, we find the best configuration at $\alpha = 2$, $t = 256$, $e = 2$, $s = 100$ and $p = 9$.

485 *Node Classification*– In the node classification experiment, we analyze both encoding distances
 486 $\alpha \in \{1, 2\}$. Other IGEL hyper-parameters are fixed after a small greedy search based on the best
 487 configurations in the link prediction experiments. For the MLP model, we perform greedy architecture
 488 search, including number of hidden units, activation functions and depth. Our results show scores
 489 averaged over five different seeded runs with the same configuration obtained from hyperparameter
 490 search.

491 The best performing hyperparameter configuration on the node classification is found with $\alpha = 2$
 492 on $t = 256$ length embedding vectors, concatenated with node features as the input layer for 1000
 493 epochs in a 3-layer MLP using ELU activations with a learning rate of 0.005. Additionally, we apply
 494 100 epoch patience for early stopping, monitoring the F1-score on the validation set.

495 *Reproducibility*– We will provide a replication folder in the code repository for the exact configurations
 496 used to run the experiments.

¹Simple 8 vertices graphs from: <http://users.cecs.anu.edu.au/~bdm/data/graphs.html>

²That is, models are not trained but simply initialized, following the approach of [20].

³Counts are normalized by the standard deviation counts across the data set for MSE values to be consistent across graphlet types, in alignment with [20].

497 H Extended Results on Isomorphism Detection and Graphlet Counting

498 In this section we summarize additional results on isomorphism detection and graphlet counting.

499 H.1 Isomorphism Detection

500 We provide a detailed breakdown of isomorphism detection performance after introducing IGEL
501 in Table 4, complimenting our summary on subsection 3.2.

502 — **Graph8c.** On the Graph8c dataset, introducing
503 IGEL significantly reduces the amount of graph pairs
504 erroneously identified as isomorphic for all MP-GNN
505 models, as shown in Table 4. Furthermore, IGEL
506 allows a linear baseline employing a sum readout
507 function over input feature vectors, then projecting
508 onto a 10-component space, to identify all but 1571
509 non-isomorphic pairs compared to the erroneous pairs
510 GCNs (4196 errors) or GATs (1827 errors) can identify
511 without IGEL. Additionally, we find that all Graph8c
512 graphs can be distinguished if the IGEL encodings for
513 $\alpha = 1$ and $\alpha = 2$ are concatenated. We do not explore
514 the expressivity of combinations of α in this work, but
515 hypothesize that concatenated encodings of α may be
516 more expressive.

517 — **Empirical Results on Strongly Regular Graphs.**
518 We also evaluate IGEL on SR25⁴, which contains 15
519 Strongly Regular graphs with 25 vertices, known to
520 be indistinguishable by 3-WL. With SR25, we vali-
521 date Theorem 1. [20] showed that no models in our
522 benchmark distinguish any of the 105 non-isomorphic
523 graph pairs in SR25. As expected from Theorem 1,
524 IGEL does not improve distinguishability.

525 H.2 Graphlet Counting

526 We evaluate IGEL on a (regression) graphlet⁵ counting task. We minimize Mean Squared Error (MSE)
527 on normalized graphlet counts⁶. Table 5 shows the results of introducing IGEL in 5 graphlet counting
528 tasks on the RandomGraph data set [33]. Stat sig. differences ($p < 0.0001$) shown in **bold green**,
529 with best (lowest MSE) per-graphlet results underlined.

530 Introducing IGEL improves counting
531 performance on triangles, tailed triangles
532 and the custom 1-WL graphlets
533 proposed by [20]. Star graphlets can
534 be identified by all baselines, and
535 IGEL only produces statistically sig-
536 nificant improvements for the Linear
537 baseline.

538 Notably, the Linear baseline plus
539 IGEL outperforms MP-GNNs without
540 IGEL for star, triangle, tailed triangle
541 and custom 1-WL graphlets. By intro-
542 ducing IGEL on the MLP baseline, it
543 outperforms all other models includ-
544 ing GNNML3 on the triangle, tailed-
545 triangle and custom 1-WL graphlets.

Table 4: Graph isomorphism detection re-
sults. The IGEL column denotes whether
IGEL is used or not in the configuration.
For Graph8c, we describe graph pairs erro-
neously detected as isomorphic. For EXP
classify, we show the accuracy of distinguish-
ing non-isomorphic graphs in a binary clas-
sification task.

Model	+ IGEL	Graph8c (#Errors)	EXP Classify (Accuracy)
Linear	No	6.242M	50%
	Yes	1571	97.25%
MLP	No	293K	50%
	Yes	1487	100%
GCN	No	4196	50%
	Yes	5	100%
GAT	No	1827	50%
	Yes	5	100%
GIN	No	571	50%
	Yes	5	100%
Chebnet	No	44	50%
	Yes	1	100%
GNNML3	No	0	100%
	Yes	0	100%

Table 5: Graphlet counting results. Cells contain mean test
set MSE error (lower is better), stat. sig **highlighted**.

Model	+ IGEL	Star	Triangle	Tailed Tri.	4-Cycle	Custom
Linear	No	1.60E-01	3.41E-01	2.82E-01	2.03E-01	5.11E-01
	Yes	4.23E-03	4.38E-03	1.85E-02	1.36E-01	5.25E-02
MLP	No	<u>2.66E-06</u>	2.56E-01	1.60E-01	1.18E-01	4.54E-01
	Yes	<u>8.31E-05</u>	5.69E-05	5.57E-05	7.64E-02	2.34E-04
GCN	No	4.72E-04	2.42E-01	1.35E-01	1.11E-01	1.54E-03
	Yes	8.26E-04	1.25E-03	4.15E-03	7.32E-02	1.17E-03
GAT	No	4.15E-04	2.35E-01	1.28E-01	1.11E-01	2.85E-03
	Yes	4.52E-04	6.22E-04	7.77E-04	7.33E-02	6.66E-04
GIN	No	3.17E-04	2.26E-01	1.22E-01	1.11E-01	2.69E-03
	Yes	6.09E-04	1.03E-03	2.72E-03	6.98E-02	2.18E-03
Chebnet	No	5.79E-04	1.71E-01	1.12E-01	8.95E-02	2.06E-03
	Yes	3.81E-03	7.88E-04	2.10E-03	7.90E-02	2.05E-03
GNNML3	No	8.90E-05	2.36E-04	2.91E-04	<u>6.82E-04</u>	9.86E-04
	Yes	9.29E-04	2.19E-04	4.23E-04	6.98E-04	4.17E-04

⁴SRG(25, 12, 5, 6) graphs from: <http://users.cecs.anu.edu.au/~bdm/data/graphs.html>

⁵3-stars, triangles, tailed triangles and 4-cycles, plus a custom 1-WL graphlet proposed in [20]

⁶Counts are stddev-normalized so that MSE values are comparable across graphlet types, following [20].

546 Since Linear and MLP baselines do not use message passing, we believe raw IGEL encodings may
547 be sufficient to identify certain graph structures even with simple linear models. For all graphlets
548 except 4-cycles, introducing IGEL yields performance similar to GNNML3 at lower pre-processing
549 and model training/inference costs, as IGEL obviates the need for costly eigen-decomposition and
550 can be used in simple models only performing graph-level readouts without message passing.

Table 6: Overview of the graphs used in the experiments. We show the average number of vertices (Avg. n), edges (Avg. m), number of graphs, target task, output shape, and splits (when applicable).

	Avg. n	Avg. m	Num. Graphs	Task	Output Shape	Splits (Train / Valid / Test)
Enzymes	32.63	62.14	600	Multi-class Graph Class.	6 (multi-class probabilities)	9-fold / 1 fold (Graphs, Train / Eval)
Mutag	17.93	39.58	188	Binary Graph Class.	2 (binary class probabilities)	9-fold / 1 fold (Graphs, Train / Eval)
Proteins	39.06	72.82	1113	Binary Graph Class.	2 (binary class probabilities)	9-fold / 1 fold (Graphs, Train / Eval)
PTC	25.55	51.92	344	Binary Graph Class.	2 (binary class probabilities)	9-fold / 1 fold (Graphs, Train / Eval)
Graph8c	8.0	28.82	11117	Non-isomorphism Detection	N/A	N/A
EXP Classify	44.44	111.21	600	Binary Class. (pairwise graph distinguishability)	1 (non-isomorphic graph pair probability)	Graph pairs 400 / 100 / 100
SR25	25	300	15	Non-isomorphism Detection	N/A	N/A
RandomGraph	18.8	62.67	5000	Regression (Graphlet Counting)	1 (graphlet counts)	Graphs 1500 / 1000 / 2500
ArXiv	18722	198110	1	Binary Class. (Link Prediction)	1 (edge probability)	Randomly sampled edges 50% train / 50% test
ASTRO-PH	4039	88234	1	Binary Class. (Link Prediction)	1 (edge probability)	Randomly sampled edges 50% train / 50% test
PPI	2373	68342.4	24	Multi-label Vertex Class.	121 (binary class probabilities)	Graphs 20 / 2 / 2